Time- And Frequency-Domain Block LMS Adaptive Digital Filters: Part Ⅱ - Performance Analysis

시간영역 및 주파수영역 블럭적응 여파기에 관한 연구 : 제 2 부 - 성능분석

Jae Chon Lee,* Chong Kwan Un*

이 재 천, 은 종 관

ABSTRACT

In Part I of the paper, we have developed various block least mean-square (BLMS) adaptive digital filters (ADF's) based on a unified matrix treatment. In Part II we analyze the convergence behaviors of the self-orthogonalizing frequency-domain BLMS (FBLMS) ADF and the unconstrained FBLMS (UFBLMS) ADF both for the overlap-save and overlap-add sectioning methods. We first show that, unlike the FBLMS ADF with a constant convergence factor, the convergence behavior of the self-orthogonalizing FBLMS ADF is governed by the same autocorrelation matrix as that of the UFBLMS ADF. We then show that the optimum solution of the UFBLMS ADF is the same as that of the constrained FBLMS ADF when the filter length is sufficiently long. The mean of the weight vector of the UFBLMS ADF is also shown to converge to the optimum Wiener weight vector under a proper condition. However, the steady-state mean-squared error (MSE) of the UFBLMS ADF turns out to be slightly worse than that of the constrained algorithm if the same convergence constant is used in both cases. On the other hand, when the filter length is not sufficiently long, while the constrained FBLMS ADF yields poor performance, the performance of the UFBLMS ADF can be improved to some extent by utilizing its extended filter-length capability. As for the self-orthogonalizing FBLMS ADF, we study how we can approximate the autocorrelation matrix by a diagonal matrix in the frequency domain. We also analyze the steady-state MSE's of the self-orthogonalizing FBLMS ADF's with and without the constraint. Finally, we present various simulation results to verify our analytical results.

요 약

본 연구의 제 1 부에서는 통일된 행렬표현 기법을 통하여 여러가지 블럭적응 여파기

* Communications Research Laboratory
Korea Advanced Institute of Science and Technology P.O. Box 150, Chongyangni Seoul, Korea.
서울 청량리 사서함 150,
한국과학기술원 통신공학연구실

보였다. 제2부에서는 여러 주파수영역 블럭적응 여파기들 중에서도 수렴속도가 매우 빠른 self-orthogonalizing 알고리즘과 계산량이 대폭 감소되는 비제약 알고리즘의 수렴특성들을 overlap-save 및 overlap-add 블럭데이타 분할방법에 대해서 분석한다. 먼저, 수렴인자가 상수일 때와는 달리, 앞에서 언급한 두 주파수영역 여파기들이 공통의 자기상관행렬의 지배를 받기 때문에 수렴특성 분석에 있어서 서로 밀접한 관련이 있음을 보인다. 다음으로 여파기 계수의 수효가 충분히 클 때, 주파수영역 블럭적응 여파기는 계수적응 알고리즘에서 제약의 유무에 관계없이 동일한 최적해를 가짐을 보인다. 그리고 나서 비제약 알고리즘의 계수들은 적절한 조건하에서 원래의 제약알고리즘과 같이 동일한 최적해에 수렴함을 증명한다. 이에 반하여, 최소자승오차 관점에서의 성능분석 결과는 제약을 풀었을 경우에 정상상태에서 약간의 성능저하가 있음을 밝혀낸다. 한편으로 계수의 수효가 작을 때는 원래의 제약 알고리즘은 심한 성능저하를 초래하는 반면에 비제약 알고리즘은 제약의 제거를 통해 상대적으로 계수의 수효가 증가된 효과 때문에 훨씬 좋은 수렴특성을 가짐을 보인다. 또한 self-orthogonalizing 주파수영역 블럭적응 여파기의 자기상관행렬이 주파수 영역에서 대각행렬로 됨을 보여 줌으로써 효율적으로 수렴시간을 단축시키는 구현방법임을 뒷받침한다.

I. INTRODUCTION

In Part I of the paper [1], we have developed various block least mean-square (BLMS) adaptive digital filters (ADF's) realized using the fast Fourier transform (FFT) and the overlap-save or overlap-add sectioning method. Among those BLMS ADF's, the self-orthogonalizing frequency-domain BLMS (FBLMS) ADF and the unconstrained FBLMS (UFBLMS) ADF have some attractive features. For example, the former has fast convergence speed, and the latter has reduced computational complexity.

The convergence properties of the BLMS ADF were studied by Clark, Mitra and Parker [2],[3]. They obtained the optimum weight vector, the condition for convergence, the time constant (or convergence speed), and the steady-state mean-squared error (MSE) [2]. These results were also compared with those of the least mean-square (LMS) ADF [4], thereby making it possible to replace easily the existing LMS ADF by the BLMS ADF which can be implemented efficiently.

The UFBLMS ADF using the overlap-save sectioning method was introduced by Mansour and Gray [5]. Based on the almost sure asymptotic exponential stability of control theory, they proved the convergence of the UFBLMS algorithm in the context of system identification. However, no analytical results were presented on the steady-state MSE. Also, by computer simulation, the self-orthogonalizing UFBLMS algorithm was shown to have fast convergence speed. In another paper [6], the convergence behaviors of the two FBLMS ADF's with and without the constraint were compared by computer simulation when the number of the filter weights is not sufficiently large.

The self-orthogonalizing FBLMS ADF based on the overlap-save sectioning method was studied by Picchi and Prati [7]. They derived the weight adjustment algorithm by minimizing the frequency-domain block MSE (BMSE) with the constraint on the frequency-domain weight vector. In order to realize the constraint, they applied the Rosen's gradient projection method [8]. However, the convergence behavior of the developed algorithm was not fully analyzed.

In Part II of the paper, we analyze the convergence behaviors of the UFBLMS ADF and the self-orthogonalizing FBLMS ADF both for the overlap-save and overlap-add sectioning methods.[1] In doing so, we inverse-

[1] We believe that the inclusion of the overlap-add case will enhance the overall understanding of the convergence behaviors of the FBLMS ADF's. However, for a coherent presentation of the results on the convergence analyses, the overlap-add case will be discussed separately in Appendix.

transform the weight vector from the frequency domain into the time domain and then follow the analysis procedure used in the LMS or BLMS case [2],[4],[9].[2] More specifically, the approach taken in our paper is as follows. We first compute the optimum Wiener solution that minimizes an appropriate performance criterion. We then derive the difference equation for the mean of the weight vector in order to prove the convergence of the underlying algorithm. From this equation, we can obtain the convergence condition and the time constants and also calculate the steady-state MSE.

Prior to detailed analysis, we investigate the differences in the mean weight-vector equations of the BLMS, self-orthogonalizing FBLMS and UFBLMS ADF's. We then study the convergence characteristics of the UFBLMS ADF's, and extend our analysis to the self-orthogonalizing algorithms. According to the results of our analysis, the optimum solutions of the two FBLMS ADF's with and without the constraint turn out to be the same when the filter length is sufficiently long. The mean of the weight vector of the UFBLMS ADF is also shown to converge to the optimum Wiener weight vector under a proper condition. On the other hand, when the filter length is not sufficiently long, the original and unconstrained FBLMS ADF's are shown to reveal quite different convergence behaviors in the steady state. As for the self-orthogonalizing FBLMS ADF, we obtain the difference equation for the mean of the weight-error vector and discuss how we can approximate the autocorrelation matrix by a diagonal matrix in the frequency domain. One of the results indicates that the self-orthogonalizing FBLMS ADF can have superior convergence speed over the self-orthogonalizing frequency-domain LMS (FLMS) ADF which operates on a sample-by-sample basis. We also obtain the analytical results on the steady-state MSE's of the self-orthogonalizing FBLMS ADF's with and without the constraint.

Following this Introduction, in Section II we briefly discuss the convergence properties of the BLMS, UFBLMS and self-orthogonalizing FBLMS ADF's. In Section III, we analyze in detail the convergence behaviors of the UFBLMS ADF. In Section IV, we study how we can realize the self-orthogonalizing algorithm in the frequency domain. In Section V, we present various simulation results to verify our analytical results. Finally, we draw conclusions in Section VI. In addition, the results of the convergence analysis of the overlap-add realization are given in Appendix.

II. CHARACTERISTICS OF BLOCK LMS ADF's

In this section, we briefly describe the properties of the BLMS, UFBLMS and self-orthogonalizing FBLMS ADF's. In our discussion, all input data for these ADF's are assumed to be stationary and real-valued. As for the BLMS ADF, a detailed convergence analysis can be found in [2]. In Sections III and IV, we compare the analytical results of the UFBLMS and self-orthogonalizing FBLMS ADF's with those of the BLMS ADF, which is reviewed in this section.

A. Optimum Block Wiener Solution and BLMS Algorithm

Assume that an FIR ADF has M weights $\{w_m\}$ and that the filter produces its output $\{y_n\}$ from the input $\{x_n\}$ and the desired response $\{d_n\}$. For our discussion here, we use the following basic equations which we used in Part I[3]:

---

[2] The reason is that, as will be seen in Sections II-IV, we can get the physical meaning of the autocorrelation matrix more easily from the time domain rather than the frequency domain view point.

[3] All the notations used in Part II will be the same as those in Part I of the paper unless otherwise stated.

Block MSE

$$ {}_B\varepsilon_k \triangleq \frac{1}{L} E[\mathbf{e}_k^t \mathbf{e}_k] \qquad (1)$$

Output vector :

$$ \mathbf{y}_k = \mathbf{X}_k \mathbf{w}_k \qquad (2a)$$

Error vector :

$$ \mathbf{e}_k = \mathbf{d}_k - \mathbf{y}_k \qquad (2b)$$

Weight vector :

$$ \mathbf{w}_{k+1} = \mathbf{w}_k + \mu \mathbf{X}_k^t \mathbf{e}_k \qquad (2c)$$

where

μ is a convergence factor.

$$ \mathbf{X}_k = \begin{bmatrix} x_{kL} & x_{kL-1} & x_{kL-2} & \cdots x_{kL-M+1} \\ x_{kL+1} & x_{kL} & x_{kL-1} & \cdots x_{kL-M+2} \\ x_{kL+2} & x_{kL+1} & x_{kL} & \cdots x_{kL-M+3} \\ \vdots & \vdots & \vdots & \vdots \\ x_{kL+L-2} & x_{kL+L-3} & x_{kL+L-4} & \cdots x_{kL-M+L-1} \\ x_{kL+L-1} & x_{kL+L-2} & x_{kL+L-3} & \cdots x_{kL-M+L} \end{bmatrix} $$

$$ \mathbf{y}_k = [y_{kL}\ y_{kL+1} \cdots y_{kL+L-1}]^t, $$

$$ \mathbf{d}_k = [d_{kL}\ d_{kL+1} \cdots d_{kL+L-1}]^t, $$

and

$$ \mathbf{w}_k = [w_{k,0}\ w_{k,1} \cdots w_{k,M-2}\ w_{k,M-1}]^t. $$

The optimum block Wiener solution that minimizes the BMSE defined in (1) can easily be obtained as the following:

$$ {}_B\mathbf{w}_{opt} = {}_B\mathbf{R}_x^{-1}\, {}_B\mathbf{p}_x \qquad (3)$$

where

$$ {}_B\mathbf{R}_x \triangleq E[\mathbf{X}_k^t \mathbf{X}_k] \text{ and } {}_B\mathbf{p}_x \triangleq E[\mathbf{X}_k^t \mathbf{d}_k] $$

When the signals are stationary, the MxM block autocorrelation matrix and Mx1 crosscorrelation vector in (3) become [2]

$$ {}_B\mathbf{R}_x = L\mathbf{R}_x \text{ and } {}_B\mathbf{p}_x = L\mathbf{p}_x \qquad (4)$$

where

$$ \mathbf{R}_x \triangleq E[\mathbf{x}_n \mathbf{x}_n^t],\quad \mathbf{p}_x \triangleq E[\mathbf{x}_n d_n], $$

$$ \text{and } \mathbf{x}_n \triangleq [x_n\ x_{n-1} \cdots x_{n-M+1}]^t. $$

Therefore, in the stationary case the block solutions are the same as the conventional Wiener solutions. That is,

$$ {}_B\mathbf{w}_{opt} = \mathbf{w}_{opt} \text{ and } {}_B\varepsilon_{min} = \varepsilon_{min} \qquad (5)$$

where $\mathbf{w}_{opt} \triangleq \mathbf{R}_x^{-1}\mathbf{p}_x$ and ε_{min} is the minimum MSE.

With the usual assumption that the signal matrix and the weight vector are uncorrelated, we can easily obtain the mean of the weight-error vector for the BLMS ADF given in (2) as the following:

$$ E[\mathbf{v}_{k+1}] = (\mathbf{I}_M - \mu\, {}_B\mathbf{R}_x) E[\mathbf{v}_k] = (\mathbf{I}_M - \mu L \mathbf{R}_x) E[\mathbf{v}_k] \qquad (6)$$

where $\mathbf{v}_k \triangleq \mathbf{w}_k - {}_B\mathbf{w}_{opt}$. Based on (6), we can obtain the convergence condition and the time constants of the MSE process, and also calculate the steady-state excess MSE as follows [2].

- Convergence condition:

$$ 0 < \mu < \frac{2}{L\lambda_{max}} \text{ or } 0 < \mu < \frac{2}{L\,tr(\mathbf{R}_x)} \qquad (7)$$

where λ_{max} is the largest value among the eigen values, $\{\lambda_i\}_{i=1}^{M}$, of $\mathbf{R}_x$.

- Time constants:

$$ {}_B\tau_i = \frac{1}{2\mu L\lambda_i} \text{ (in blocks)} \qquad (8a)$$

$$ = \frac{1}{2\mu\lambda_i} \text{ (in samples)},\ 1 \le i \le M, \qquad (8b)$$

- Excess MSE:

$$ {}_B\varepsilon_{ex} = \frac{1}{2}\mu\, tr({}_B\mathbf{R}_x / L)\, {}_B\varepsilon_{min} $$

$$ = \frac{1}{2}\mu\, tr(\mathbf{R}_x)\, \varepsilon_{min} = \frac{1}{2}\mu M \sigma_x^2 \varepsilon_{min} \qquad (9)$$

were $tr(R_x)$ denotes the sum of the diagonal elements of R_x and $\sigma_x^2 \triangleq E[x_n^2]$

It is noted here that, since both the TBLMS and FBLMS ADF's using a constant convergence factor μ are exact implementations of the BLMS ADF, they have the same convergence characteristics as those of the BLMS ADF.

B. Unconstrained FBLMS Algorithm

In Part I of the paper, we have discussed two FBLMS algorithms based on the overlap-save sectioning which are given as

$$ {}_s\boldsymbol{\omega}_{k+1} = {}_s\boldsymbol{\omega}_k + \mu \boldsymbol{P}_{M,0}\ {}_s\overline{\boldsymbol{X}}_k\ {}_s\boldsymbol{e}_k \tag{10a} $$

and

$$ {}_s\boldsymbol{\omega}_{k+1} = \boldsymbol{P}_{M,0}\ ({}_s\boldsymbol{\omega}_k + \mu\, {}_s\overline{\boldsymbol{X}}_k\ {}_s\boldsymbol{e}_k). \tag{10b} $$

It should be noted that the FBLMS algorithm in (10a) is an exact implementation of the BLMS algorithm in (2c), whereas the FBLMS algorithm in (10b) is not. Expecially, they have different convergence behaviors in the sense that, unlike the latter algorithm, the former algorithm converges to the optimum solution only for a special initial condition (i.e., $\boldsymbol{P}_{M,0}\ {}_s\boldsymbol{\omega}_0 = {}_s\boldsymbol{\omega}_0$) As will be seen in Sections III-V, when the filter length is sufficiently long, the UFBLMS algorithm has the same convergence characteristics as those of the FBLMS algorithm in (10b). For this reason, hereafter we represent the UFBLMS and FBLMS algorithms using new frequency-domain vectors ${}_u\boldsymbol{\omega}_k$ and ${}_u\boldsymbol{e}_k$ as follows.

UFBLMS:

$$ {}_u\boldsymbol{\omega}_{k+1} \triangleq {}_u\boldsymbol{\omega}_k + \mu\, {}_s\overline{\boldsymbol{X}}_k\ {}_u\boldsymbol{e}_k . \tag{11} $$

FBLMS :

$$ {}_s\boldsymbol{\omega}_{k+1} \triangleq \boldsymbol{P}_{M,0}\ ({}_s\boldsymbol{\omega}_k + \mu\, {}_s\overline{\boldsymbol{X}}_k\ {}_s\boldsymbol{e}_k). \tag{12} $$

In (11), the frequency-domain error vector of the UFBLMS ADF is given from (33) of Part I as

$$ {}_u\boldsymbol{e}_k = {}_s\boldsymbol{d}_k - \boldsymbol{P}_{0,L}\ {}_s\boldsymbol{X}_k\ {}_u\boldsymbol{\omega}_k \tag{13} $$

Let us discuss the convergence behavior of the UFBLMS algorithm of (11) in terms of the mean weight vector. Substituting (13) into (11) and taking expectation of both sides of (11) lead to

$$ E[{}_u\boldsymbol{\omega}_{k+1}] = E[{}_u\boldsymbol{\omega}_k] + \mu \{ E[{}_s\overline{\boldsymbol{X}}_k\ {}_s\boldsymbol{d}_k] - E[{}_s\overline{\boldsymbol{X}}_k\ \boldsymbol{P}_{0,L}\ {}_s\boldsymbol{X}_k]\ E[{}_u\boldsymbol{\omega}_k] \}. \tag{14} $$

In order to see the difference in the convergence behaviors between the BLMS and UFBLMS ADF's, we inverse-transform both sides of (14) and obtain

$$ E[{}_u\mathbf{w}_{k+1}] = E[{}_u\mathbf{w}_k] + \mu \{ E[{}_s\mathbf{X}_u^t\, \mathbf{d}_k] - E[{}_s\mathbf{X}_u^t\ {}_s\mathbf{X}_u]\ E[{}_u\mathbf{w}_k] \} \tag{15} $$

where ${}_u\mathbf{w}_k = \mathbf{F}^{-1}\ {}_u\boldsymbol{\omega}_k$ In (15), the LxN matrix ${}_s\boldsymbol{X}_u$ is a part of the NxN circulant matrix ${}_s\mathbf{X}_k$ and they are defined from (5) of Part I as

$$ {}_s\mathbf{X}_k \triangleq \begin{array}{c} \left[\begin{array}{c:c} \mathbf{X}_a & \mathbf{X}_b \\ \hdashline \mathbf{X}_k & \mathbf{X}_c \end{array} \right] \begin{array}{l} N-L \\ L \end{array} \\ \begin{array}{cc} M & N-M \end{array} \end{array} \quad \text{and} \quad {}_s\mathbf{X}_u \triangleq [\mathbf{X}_k \ \vdots\ \mathbf{X}_c] \tag{16} $$

It should be noted here that the size of the time-domain weight vector ${}_u\mathbf{w}_k$ in (15) is Nx1, while the size of $\mathbf{w}_k$ in (2c) is Mxl. As can be seen from (6) and (15), unlike the BLMS ADF, the time-domain autocorrelation matrix of the UFBLMS algorithm is given by $E[{}_s\mathbf{X}_u^t\ {}_s\mathbf{X}_u]$ whose size is NxN. The characteristics of this new autocorrelation matrix will be studied in detail in Sections III and IV.

C. Self-orthogonalizing FBLMS Algorithm

Following the same point of view presented in the previous subsection, two self-orthogonalizing FBLMS algorithms using the overlap-save sectioning method can be considered as the following:

$$ {}_u\boldsymbol{\omega}_{k+1} = {}_u\boldsymbol{\omega}_k + \gamma\, {}_s\boldsymbol{R}_k^{-1}\ {}_s\overline{\boldsymbol{X}}_k\ {}_u\boldsymbol{e}_k \tag{17a} $$

and

$$ {}_s\boldsymbol{\omega}_{k+1} = \boldsymbol{P}_{M,0}\,({}_s\boldsymbol{\omega}_k + \gamma\,{}_s\boldsymbol{R}_k^{-1}\,{}_s\bar{\boldsymbol{X}}_k\,{}_s\boldsymbol{e}_k), \qquad (17b) $$

where ${}_s\boldsymbol{R}_k$ is an NxN diagonal matrix which can be estimated using some appropriate method [for example, see (46) of Part I] in actual realization of (17). Here, we discuss the characteristics of the self-orthogonalizing version of the constrained algorithm in (17b). Inserting (13) into (17b), we can obtain the mean of the frequency-domain weight vector as

$$ E[{}_s\boldsymbol{\omega}_{k+1}] = \boldsymbol{P}_{M,0}\,E[{}_s\boldsymbol{\omega}_k] + \gamma\,\boldsymbol{P}_{M,0}\,{}_s\boldsymbol{R}_k^{-1} \{E[{}_s\bar{\mathbf{X}}_k\,{}_s\boldsymbol{d}_k] - E[{}_s\bar{\mathbf{X}}_k\,\boldsymbol{P}_{0,1}\,{}_s\mathbf{X}_k]\,\boldsymbol{P}_{M,0}\,E[{}_s\boldsymbol{\omega}_k]\}. \qquad (18) $$

Noting that the last (N-M) elements of the inverse transform of ${}_s\boldsymbol{\omega}_k$ are zero, we can get from (18)

$$ E[\mathbf{w}_{k+1}] = E[\mathbf{w}_k] + \gamma\,\mathbf{P}_{M}\,(\mathbf{F}^{-1}\,{}_s\boldsymbol{R}_k^{-1}\,\mathbf{F}) \{E[{}_s\mathbf{X}_u^t\,\mathbf{d}_k] - E[{}_s\mathbf{X}_u^t\,\mathbf{X}_k]\,E[\mathbf{w}_k]\}. \qquad (19) $$

Comparing (15) and (19), one can see that the time-domain autocorrelation matrix of the self-orthogonalizing algorithm is not the same in its present form as that of the UFBLMS algorithm. However, we can show from (16) that, since ${}_s\mathbf{X}_u = [\mathbf{X}_k \; \mathbf{X}_c]$ we have for the last term in (19)

$$ E[{}_s\mathbf{X}_u^t\,\mathbf{X}_k]\,E[\mathbf{w}_k] = E[{}_s\mathbf{X}_u^t\,{}_s\mathbf{X}_u] \begin{bmatrix} E[\mathbf{w}_k] \\ 0 \end{bmatrix} \begin{matrix} M \\ N-M \end{matrix} \qquad (20) $$

Thus, the convergence behavior of the self-orthogonalizing FBLMS ADF is governed by the same NxN matrix $E[{}_s\mathbf{X}_u^t\,{}_s\mathbf{X}_u]$ as that of the UFBLMS ADF. For this reason, in next sections we analyze the convergence behavior of the UFBLMS ADF first and then extend our analysis to the self-orthogonalizing FBLMS ADF. It is noted that, when the matrix ${}_s\boldsymbol{R}_k$ is an identity matrix, the difference equation of (19) becomes that of the BLMS ADF in (6). Note also from (6) and (19) that the use of the diagonal matrix in the frequency domain introduces another input matrix $\mathbf{X}_c'$ which does not appear in the weight vector equation of the BLMS ADF. The effec of $\mathbf{X}_c$ on the convergence behavior will be studied in Section IV. The convergence behavior of the self-orthogonalizing version for the UFBLMS ADF will also be analyzed in that section.

III. CONVERGENCE-ANALYSIS OF UNCENSTRAINED FBLMS ADF's

As can be seen in (3), the optimum Wiener weights are completely determined in the time domain by the autocorrelation values of the input signal and the crosscorrelation values between the desired and input signals. Alternatively, they are determined in the frequency domain by the power spectra of the input and desired signals. It is known that, unless the bandwidth of the frequency spectrum is extremely narrow like a tone, the effective duration of the inverse transform of the spectrum which is of finite bandwidth in the frequency domain is also finite. Therefore, in most applications of the ADF in which the signal spectra are of finite bandwidth, both the correlation values and optimum filter weights approach zero when they are sufficiently far away from the center of the time origin. In this case, the optimum Wiener filter can be approximated by a finite impulse response (FIR) filter. Based on this FIR approximation, we can represent the desired signal as

$$ d_n = \sum_{i=0}^{M_o-1} x_{n-i}\,w_{o,i} + \xi_n \qquad (21) $$

where M_o is the number of the model filter weights, $\{w_{o,i}\}$ and $\{\xi_n\}$ is a zero-mean white noise process that is uncorrelated with $\{x_n\}$. It is noted that the accuracy of the approximation can be arbitrarily improved by increasing M_o. Consequently, in realization of the system whose signals are modeled by (21), the number of the weights of the ADF, M, must be greater than or equal to M_o to achieve the best performance. It can easily be shown that under the signal model of(21)with $M=M_o$, the optimum Wiener weight vector becomes the model weight vector ${}_{B}\mathbf{w}_{opt}=\mathbf{w}_{opt}=\mathbf{w}_d \triangleq [w_{d,0}, w_{d,1}, \cdots, w_{d,M-1}]^t$ In the following, we analyze the convergence behavior of the UFBLMS ADF first when $M=M_o$ and then discuss how the convergence behavior will be changed when $M<M_o$

In the UFBLMS algorithm, there is no constraint on the weight vector. Therefore, unlike in the constrained algorithm, all the N elements of the time-domain weight vector are used in computing the output and adjusting the weights. To see this aspect more clearly, from (13) and (15) we represent the output and adjustment algorithm of the UFBLMS ADF in the time domain as

$$\mathbf{y}_k={}_s\mathbf{X}_u\,{}_u\mathbf{w}_k \tag{22a}$$

and

$${}_u\mathbf{w}_{k+1}={}_u\mathbf{w}_k+\mu\,{}_s\mathbf{X}_u^t\,\mathbf{e}_k. \tag{22b}$$

By splitting into

$${}_u\mathbf{w}_k \triangleq \begin{bmatrix} {}_a\mathbf{w}_k \\ {}_b\mathbf{w}_k \end{bmatrix} \begin{matrix} M \\ N-M \end{matrix}, \tag{23}$$

we decompose (22) as the following:

$$\mathbf{y}_k=\mathbf{X}_k\,{}_a\mathbf{w}_k+\mathbf{X}_c\,{}_b\mathbf{w}_k, \tag{24a}$$

$${}_a\mathbf{w}_{k+1}={}_a\mathbf{w}_k+\mu\,\mathbf{X}_k^t\,\mathbf{e}_k, \tag{24b}$$

$${}_b\mathbf{w}_{k+1}={}_b\mathbf{w}_k+\mu\,\mathbf{X}_c^t\,\mathbf{e}_k, \tag{24c}$$

One can see from (24) that removing the constraint on the weights introduces additional terms, which are related with $\mathbf{X}_c$ in the output and adjustment algorithm. Since $\mathbf{X}_c$ is generated by circular extension of $\mathbf{X}_k$, the additional terms incurred above have been called the circular convolution effect. In the following, we investigate how the circular convolution terms affect the convergence behavior. We first compute the optimum solution and the mean of the weight vector of the UFBLMS algorithm. We then obtain various results on the convergence behavior.

A. UFBLMS Algorithm and Its Optimum Solution

The optimum weight vector of the UFBLMS ADF is derived by minimizing the unconstrained frequency-domain BMSE. Alternatively, we can obtain the same solution based on the block orthogonality principle [2]. According to this principle and from (11), the optimum weight vector, ${}_u\omega_{opt}$ must satisfy

$$E[{}_s\bar{\mathbf{X}}_k\,{}_u\mathbf{e}_k]=\mathbf{O}. \tag{25}$$

We get from (25) the equation for the optimum weight vector as

$$E[{}_s\bar{\mathbf{X}}_k\,{}_s\mathbf{d}_k]=E[{}_s\bar{\mathbf{X}}_k\,\mathbf{P}_{0,1}\,{}_s\mathbf{X}_k]\,{}_u\omega_{opt} \tag{26a}$$

or

$$E[{}_s\mathbf{X}_u^t\,\mathbf{d}_k]=E[{}_s\mathbf{X}_u^t\,{}_s\mathbf{X}_u]\,{}_u\mathbf{w}_{opt}. \tag{26b}$$

Also, combining (26b) and (15), we obtain the expression for the mean of the weight-error vector as

$$E[{}_u\mathbf{v}_{k+1}]=(\mathbf{I}_N-\mu\,{}_u\mathbf{R}_x)\,E[{}_u\mathbf{v}_k] \tag{27}$$

where ${}_u\mathbf{v}_k \triangleq {}_u\mathbf{w}_k-{}_u\mathbf{w}_{opt}$ and ${}_u\mathbf{R}_x \triangleq E[{}_s\mathbf{X}_u^t\,{}_s\mathbf{X}_u]$. Thus, we can see from (26b) and (27) that depending on the properties of the matrix ${}_u\mathbf{R}_x$, the UFBLMS ADF can have a unique optimum weight vector and also the weight vector of the filter can converge in the mean to the optimum solution independently of the initial value of the weight vector ${}_u\mathbf{w}_0$ (or ${}_u\omega_0$).
In the next subsection, we investigate the properties of ${}_u\mathbf{R}_x$

B. Properties of the Autocorrelation Matrix ${}_uR_x$

Based on (16), we can decompose ${}_uR_x$ as

$$
{}_uR_x = E[{}_sX_u^t\,{}_sX_u] = \begin{bmatrix} E[X_k^t X_k] & E[X_k^t X_c] \\ E[X_c^t X_k] & E[X_c^t X_c] \end{bmatrix}
$$

$$
= \begin{array}{c} \begin{bmatrix} {}_BR_x & R_\ell^t \\ R_\ell & R_c \end{bmatrix} \begin{matrix} M \\ N-M \end{matrix} \\ \begin{matrix} M \quad & N-M \end{matrix} \end{array} \qquad (28)
$$

It is noted from (28) that ${}_uR_x$ is an NxN symmetric matrix. To evaluate ${}_uR_x$, we have to specify the elements of the L x (N-M) matrix which is the lower-right part of the NxN circulant matrix ${}_sX_k$. For the ease of analysis, N_z is assumed to be zero for which case N=L+M-1. In this case, X_c is given as

$$
X_c = \begin{bmatrix} x_{kL+L-1} & x_{kL+L-2} & \cdots x_{kL+2} & x_{kL+1} \\ x_{kL+M-1} & x_{kL+L-1} & \cdots x_{kL+3} & x_{kL+2} \\ x_{kL+M-2} & x_{kL+M-1} & \cdots x_{kL+4} & x_{kL+3} \\ \vdots & \vdots & \vdots & \vdots \\ x_{kL+M-L+2} & x_{kL+M-L+3} & \cdots x_{kL+M-1} & x_{kL+L-1} \\ x_{kL+M-L+1} & x_{kL+M-L+2} & \cdots x_{kL+M-2} & x_{kL+M-1} \end{bmatrix} \qquad (29)
$$

Defining the correlation of the stationary input process as $\rho_\ell \triangleq E[x_n x_{n-\ell}]$, from (2) and (29) we can compute all the elements of the submatrices ${}_BR_x$, R_c and R_ℓ as the following[4]:

$$({}_BR_x)_{i,j} = L\rho_{i-j}, \quad \text{where } 1 \leq i, j \leq M, \qquad (30a)$$

$$(R_c)_{i,j} = (L-|i-j|)\rho_{i-j} + |i-j|\rho_{N-|i-j|},$$

$$\text{where } 1 \leq i, j \leq N-M, \qquad (30b)$$

$$(R_\ell)_{i,j} = [\text{illegible}]\,\rho_{N-M-i+j} + [\text{illegible}]\,(N-M-[\text{illegible}])\,\rho_{[\text{illegible}]},$$

$$\text{where } 1 \leq i \leq N-M \text{ and } 1 \leq j \leq M \qquad (30c)$$

It is noted from (30) that, unlike the matrix R_ℓ, both matrices ${}_BR_x$ and R_c are symmetric Toeplitz. When ρ_ℓ is very small for ℓ greater than a positive integer m, we can neglect those terms in the above matrices When M is sufficiently greater than m, ${}_BR_x$ reduces to

$$
{}_BR_x = LR_x = L\begin{bmatrix} \rho_0 & \rho_1 & \rho_2 & \cdots \rho_m & & 0 \\ \rho_1 & \rho_0 & \rho_1 & \ddots & \ddots & \\ \rho_2 & \rho_1 & \rho_0 & \ddots & \ddots & \rho_m \\ \vdots & \ddots & \ddots & \ddots & \ddots & \vdots \\ \rho_m & & \ddots & \rho_0 & \rho_1 & \rho_2 \\ & \ddots & & \ddots & \rho_1 & \rho_0 & \rho_1 \\ 0 & & \rho_m & \cdots \rho_2 & \rho_1 & \rho_0 \end{bmatrix} \qquad (31a)
$$

when $M \gg m$, N is also far greater than m. In that case, one of two correlation terms both in (30b) and (30c) can be neglected. Thus, we get from (30b) and (30c)

$$
R_c = L\begin{bmatrix} a_0\rho_0 & a_1\rho_1 & a_2\rho_2 & \cdots a_m\rho_m & & & 0 \\ a_1\rho_1 & a_0\rho_0 & a_1\rho_1 & \ddots & \ddots & & \\ a_2\rho_2 & a_1\rho_1 & a_0\rho_0 & \ddots & \ddots & \ddots & \\ \vdots & \ddots & \ddots & \ddots & \ddots & \ddots & \\ a_m\rho_m & & \ddots & \ddots & \ddots & \ddots & a_m\rho_m \\ & \ddots & & \ddots & \ddots & \ddots & \vdots \\ & & \ddots & & a_0\rho_0 & a_1\rho_1 & a_2\rho_2 \\ 0 & & & \ddots & a_1\rho_1 & a_0\rho_0 & a_1\rho_1 \\ & & & a_m\rho_m \cdots & a_2\rho_2 & a_1\rho_1 & a_0\rho_0 \end{bmatrix}
$$

and

4 When N_z is not zero, though (30b) and (30c) must be slightly modified, the general structure will still be maintained. Also, in that case, for a better approximation of ${}_uR_x$ it may be preferable to use N_z previous input data instead of zero-valued data [see the footnote 3 of Part I].

$$R_l = L\begin{bmatrix} & & & & a_1\rho_m \cdots a_1\rho_4 & a_1\rho_3 & a_1\rho_2\; a_1\rho_1 \\ & & & & \ddots & \ddots & a_2\rho_3\; a_2\rho_2 \\ & & & & & \ddots & a_3\rho_3 \\ a_m\rho_m & & & & & \ddots & a_4\rho_4 \\ \vdots & \ddots & & 0 & & & \vdots \\ a_4\rho_4 & & \ddots & & & & a_m\rho_m \\ a_3\rho_3 & \ddots & & \ddots & & & \\ a_2\rho_2\; a_2\rho_3 & & \ddots & & \ddots & & \\ a_1\rho_1\; a_1\rho_2 & a_1\rho_3 & a_1\rho_4 \cdots a_1\rho_m & & & & \end{bmatrix} \tag{31c}$$

where

$$a_l \triangleq 1-\frac{l}{L}, \quad 0 \leqq l \leqq m.$$

When L is sufficiently larger than m, all a_l's can be approximated as unity. In that case the NxN matrix ${}_uR_x$ becomes from (31)

$${}_uR_x = L\left[\begin{array}{ccccc|ccccc} \rho_0 & \rho_1 & \rho_2 & \cdots & \rho_m & & & \rho_m & \cdots \rho_2 & \rho_1 \\ \rho_1 & \rho_0 & \rho_1 & \ddots & \ddots & & & & \ddots & \rho_2 \\ \rho_2 & \rho_1 & \rho_0 & \ddots & \ddots & & & & & \vdots \\ \vdots & \ddots & \ddots & \ddots & \rho_m & & & & & \rho_m \\ \rho_m & \ddots & \ddots & \ddots & \ddots & \rho_m & & 0 & & \\ & \ddots & \rho_0 & \rho_1 & \rho_2 & \ddots & \ddots & & & \\ & & \rho_1 & \rho_0 & \rho_1 & \rho_2 & & \ddots & & \\ \rho_m & \cdots & \rho_2 & \rho_1 & \rho_0 & \rho_1 & \rho_2 & \cdots & \rho_m & \\ \hline \rho_m & \cdots & \rho_2 & \rho_1 & & \rho_0 & \rho_1 & \rho_2 & \cdots & \rho_m \\ & & & \rho_2 & & \rho_1 & \rho_0 & \rho_1 & \ddots & \\ & & & & & \rho_2 & \rho_1 & \rho_0 & \ddots & \ddots \\ & & & \rho_m & & & \ddots & \ddots & \ddots & \\ & & 0 & & & \rho_m & & \ddots & \ddots & \rho_m \\ \rho_m & & & & & & \ddots & & & \vdots \\ \vdots & & & & & & & \rho_0 & \rho_1 & \rho_2 \\ \rho_2 & & & & & & & \rho_1 & \rho_0 & \rho_1 \\ \rho_1 & \rho_2 & \cdots & \rho_m & & & \rho_m & \cdots & \rho_2\;\rho_1 & \rho_0 \end{array}\right] \tag{32}$$

Consequently, we can see from (32) that, when $m \ll M$ and $m \ll L$, ${}_uR_x$ becomes an NxN circulant matrix. It is known that a circulant matrix is diagonalized by the discrete Fourier transform (DFT) [10]. Thus, we get the eigenvalues $\{\lambda_i\}_{i=1}^{M}$ of ${}_uR_x/L$ as follows [11]

$${}_uR_x/L = F^{-1}\,{}_u\Lambda_x\, F = (F/\sqrt{N})^{-1}\,{}_u\Lambda_x\,(F/\sqrt{N}) \tag{33}$$

where F is the NxN DFT matrix and the NxN diagnal matrix ${}_u\Lambda_x$ is defined by ${}_u\Lambda_x \triangleq \mathrm{diag}({}_u\lambda_1, {}_u\lambda_2, \cdots, {}_u\lambda_{N-1}, {}_u\lambda_N)$. In (33), $\{{}_u\lambda_i\}$ are determined by the DFT of the first column of ${}_uR_x/L$ as the following:

$${}_u\lambda_i = \sum_{l=0}^{m} \rho_l \exp[-j2\pi l(i-1)/N] + \sum_{l=1}^{m} \rho_l \exp[-j2\pi(N-l)(i-1)/N] \tag{34}$$

$$= \rho_0 + 2\sum_{l=1}^{m} \rho_l \cos[2\pi l(i-1)/N], \quad 1 \leqq i \leqq N.$$

On the other hand, when $m \ll M$, the MxM matrix ${}_BR_x$ can be approximated by an MxM circulant matrix as was done in [9]. In that case, we get the eigenvalues $\{\lambda_i\}_{i=1}^{M}$ of ${}_BR_x/L$ as the following:

$$\lambda_i = \sum_{l=0}^{m} \rho_l \exp[-j2\pi l(i-1)/M] + \sum_{l=1}^{m} \rho_l \exp[-j2\pi(M-l)(i-1)/M] \tag{35}$$

$$= \rho_0 + 2\sum_{l=1}^{m} \rho_l \cos[2\pi l(i-1)/M], \quad 1 \leqq i \leqq M.$$

It is noted from (34) and (35) that $\{\lambda_i\}_{i=1}^{M}$ and $\{{}_u\lambda_i\}_{i=1}^{N}$ represent the M-point and N-point, respectively, power spectra of the same input random process $\{x_n\}$. For example, when N=2M, the even-numbered frequency components (or eigenvalues) of ${}_uR_x$ are the same as those of ${}_BR_x$, i.e., ${}_u\lambda_{2i} = \lambda_i$, $1 \leqq i \leqq M$ [see (34) and (35)]. The odd-numbered ones are generated by interpolating the values $\{\lambda_i\}$. Thus, if $M \gg m$, the M-point power spectrum already has sufficient frequency resolution because the number of zeros appended is N-(2m+1). Hence, even in the N-point power spectrum which has increased frequency resolution, there will be no spurious peaks and valleys which did not appear in the M-point spectrum. Therefore, we can see that the eigenvalue distributions of the two matrices

${}_{u}\mathbf{R}_x$ and ${}_{B}\mathbf{R}_x$ are asymptotically the same except for the different number of eigenvalues. For example, ${}_{u}\lambda_{max} \cong \lambda_{max}$ and ${}_{u}\lambda_{min} \cong \lambda_{min}$

C. Convergence Properties of UFBLMS Algorithm

We are now ready to solve the optimum solution and study the convergence behaviors of the UFBLMS ADF. According to the results obtained in the previous subsection, the matrix ${}_{u}\mathbf{R}_x$ is nonsingular as ${}_{B}\mathbf{R}_x$ is nonsingular. Thus, we can solve (26b) for ${}_{u}\mathbf{w}_{opt}$ However, our concern here is how the Nxl weight vector ${}_{u}\mathbf{w}_{opt}$ is related to the Mxl weight vector ${}_{B}\mathbf{w}_{opt}$. Based on the signal model in (21) and when $M = M_o$, we can show that

$$\mathbf{d}_k = \mathbf{X}_k \mathbf{w}_d + \boldsymbol{\xi}_k \tag{36}$$

where

$$\boldsymbol{\xi}_k \triangleq [\xi_{kL}\ \xi_{kL+1} \cdots \xi_{kL+L-1}]^t$$

Inserting (36) into (26b) yields

$${}_{u}\mathbf{R}_x\, {}_{u}\mathbf{w}_{opt} = E[{}_{s}\mathbf{X}_u^t\, \mathbf{X}_k]\, \mathbf{w}_d = E[{}_{s}\mathbf{X}_u^t\, \mathbf{X}_k]\, {}_{B}\mathbf{w}_{opt}. \tag{37}$$

Splitting the Nxl vector ${}_{u}\mathbf{w}_{opt}$ into two subvectors ${}_{a}\mathbf{w}_{opt}$ and ${}_{b}\mathbf{w}_{opt}$, we get from (37)

$${}_{u}\mathbf{R}_x \begin{bmatrix} {}_{a}\mathbf{w}_{opt} - {}_{B}\mathbf{w}_{opt} \\ \cdots\cdots\cdots \\ {}_{b}\mathbf{w}_{opt} \end{bmatrix}\begin{matrix} M \\ \\ N-M \end{matrix} = 0. \tag{38}$$

Thus, we obtain from (38) the optimum solution of the UFBLMS ADF as

$${}_{a}\mathbf{w}_{opt} = {}_{B}\mathbf{w}_{opt} \quad \text{and} \quad {}_{b}\mathbf{w}_{opt} = 0. \tag{39}$$

Also, one can see from (39) that the minimum MSE of the UFBLMS ADF, ${}_{u}\varepsilon_{min}$, is the same as that of the BLMS ADF, ${}_{B}\varepsilon_{min}$ The optimum solution of (39) indicates that when $M \geq M_o$, no circular convolution effect occurs even without the constraining operation on the weights. This is another unique feature of the ADF compared to the fixed-coefficient digital filter. It has already been shown in [12] that, unlike in fixed-coefficient digital filtering, the overlap-save implementation requires less computation for the BLMS ADF than the overlap-add implementation. Adaptive realization of an ADF using appropriate desired signals enables the self-constraining operation.

We can get from (27) and Section III-B the convergence properties of the UFBLMS ADF as follows.

- Convergence condition:

$$0 < \mu < \frac{2}{L\, {}_{u}\lambda_{max}} \quad \text{or} \quad 0 < \mu < \frac{2}{L\, tr\, ({}_{u}\mathbf{R}_x)} \tag{40}$$

- Time constants:

$${}_{u}\tau_i = \frac{1}{2\mu\, {}_{u}\lambda_i} \text{ (in samples)}, \quad 1 \leq i \leq N \tag{41}$$

- Excess MSE:

$${}_{u}\varepsilon_{\Delta} = \frac{1}{2}\, tr\, ({}_{u}\mathbf{R}_x / L)\, {}_{u}\varepsilon_{min} = \frac{1}{2} \mu N \sigma_x^2 \varepsilon_{min}. \tag{42}$$

Comparing (9b) and (42), one can see that the UFBLMS ADF can save two FFT operations at the expense of the slightly increased steady-state MSE when the same convergence constants are used in both cases. As will be seen in Section V, this increase is not significant. For example, according to (9b) and (42), the difference in the steady-state MSE's between the two cases is about 0.3 dB when $\mu = 0.01$, M=16, N=32, and $\sigma_x^2 = 1$.

D. Circular Convolution Effect

So far we have discussed the convergence behaviors of the UFBLMS ADF when $M \geq M_o$. Here, we consider the case when $M < M_o$. It is clear that, when $M < M_o$, the optimum solution of the BLMS ADF, ${}_{B}\mathbf{w}_{opt}$, is a truncated version of $\mathbf{w}_d$. Also, ${}_{B}\varepsilon_{min}$ increases because of the truncation of the optimum weight vector. In the following, we are going to discuss how the UFBLMS ADF works in this situation. The output of the UFBLMS ADF is given from (22a) and (23) as

$$y_k = {}_sX_u\,{}_uw_k = [\,X_k \ \vdots\ X_c\,]\begin{bmatrix} {}_aw_k \\ \cdots \\ {}_bw_k \end{bmatrix}\begin{matrix} M \\ \\ N-M \end{matrix} \tag{43}$$

It is noted from (29) that, since X_c is the circular extension of X_k, in each row of X_c there is a jump in the time indices of the input data $\{x_n\}$. To see the effect of the assumption on $M < M_o$, we schematically draw the matrix ${}_sX_u$ and the vector ${}_uw_k$ in Fig. 1. In Fig. 1 the jump is represented by the diagonal solid line in X_c. As can be seen in Fig. 1, in the BLMS ADF, only the first $M\,(<M_o)$ elements of the time-domain weight vector can have nonzero values. Recalling the results in the previous subsections, the UFBLMS ADF in this situation will try to optimize its performance by utilizing the first $M_o(>M)$ elements of the vector, while the last $N-M_o$ elements will approach zero values. It is, therefore, important to see how the M_o-M weights, ${}_ew_k$, in the middle of ${}_uw_k$ in Fig. 1 affects the convergence behavior of the UFBLMS ADF. One can see from Fig. 1 that the matrix $\tilde{\tilde{X}}_k$ with its size $(L-(M_o-M))\times M_o$ becomes the lower part of X_k when $M < M_o$. As for the matrix $\tilde{X}_k$ with its size $(M_o-M)\times M_o$, the time index of the data in the last M_o-M columns is not continuous, and particulary in each row of $\tilde{X}_k$ two data being apart by N sampling times are undesirably wrapped around. Therefore, the existence of non-zero ${}_ew_k$ will help improve the performance in the last $L-(M_o-M)$ output samples, whereas in the first M_o-M output samples it will not. However, to reduce the overall block MSE, the $M_o\times 1$ weight vector $\bar{w}_k \triangleq [\,{}_Bw_k^t \ \vdots\ {}_ew_k^t\,]^t$ will try to be close to the optimum weight vector, ${}_Bw_{opt}$ for the case of $M=M_o$. It can also be seen that, unlike for the first M_o-M output samples, the MSE of the UFBLMS ADF for the last $L-(M_o-M)$ output samples will be significantly improved compared to that of the BLMS ADF. All these phenomena will be demonstrated by computer simulation in Section V.

It can be seen from Fig. 1 that, given M_o, the undesirable wrap-around (or circular convolution) effect increases and propagates from the first output sample toward the last output sample in each block as M decreases to 1. Thus,

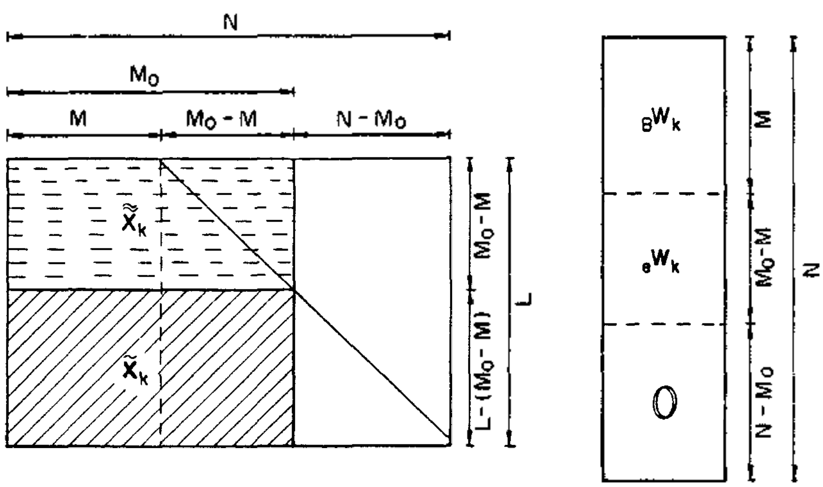

(a) (b)

Fig. 1. A schematic representation of the circular convolution effect when $M < M_o$.
(a) ${}_sX_u = [\,\underbrace{X_k}_{M}\ \ \underbrace{X_c}_{N-M}\,]\ L$.
(b) ${}_uw_k \triangleq [\,\underbrace{{}_Bw_k^t}_{M}\ \ \underbrace{{}_ew_k^t}_{M_o-M}\ \ \underbrace{0^t}_{N-M_o}\,]^t$

unless the input has special characteristics (for example, periodicity) to avoid the wrap-around effect. the worst performance of the UFBLMS ADF yields when M=1. Assuming $N_{\Delta}=0$ we can easily see that the case with M=1 leads to a special structure of the UFBLMS ADF in which N=L. In addition to the removed constraint in weight adjustment, the sectioning operation for computing the output is also eliminated in this structure since $P_{0,1} = I_N$ and thus $y_k = F^{-1}({}_sX_k\,{}_u\omega_k)$. This UFBLMS ADF is the same as the structure studied in [13]-[18]. As discussed above, this structure cannot be expected to show good performance in most applications because of the serious wrap-around effect. One possible use of the UFBLMS ADF with M=1 would be in the adaptive line enhancement (ALE) application. According to our results of computer simulation, even in the ALE, this structure appears not to show good performance unless the time lag N-1 is some multiple of the period (in samples) of the input sinusoid and the signal-to-noise ratio (SNR) is high. In Section V, we will also present some results of computer simulation, illustrating the performance characteristics of the UFBLMS ADF in Δ-step linear prediction applications. According to these results, the first M elements of the time-domain weight vector of the UFBLMS ADF have the same information about the signals as that of the constrained algorithm.

IV. CONVERGENCE ANALYSIS OF SELF-ORTHOGONALIZING FBLMS ADF's

The self-orthogonalizing algorithms of the LMS-type ADF's have been known to have fast convergence speed without altering the optimum Wiener solution [19]. In this section. we first discuss how we can implement in the frequency domain some self-orthogonalizing algorithms for the UFBLMS ADF and then extend our discussion to the constrained algorithm.

A. Self-orthogonalizing Agorithms for UFBLMS ADF

In Section III. we have shown that the convergence behavior of the UFBLMS ADF is governed by the matrix ${}_uR_x$ and it can be approximated as a circulant matrix which is diagonalized by the DFT. Since the inverse of a circulant matrix can be computed relatively easily in the DFT domain. we can consider a self-orthogonalizing algorithm in which the mean of the weight-error vector is given as [9],[19]

$$E[{}_uv_{k+1}] = (I_N - \eta L\,{}_uR_x^{-1}\,{}_uR_x)\,E[{}_uv_k] \qquad (44)$$

when is a convergence constant. Referring to the approach taken in Section III-A, we can derive the UFBLMS algorithm which corresponds to (44) as the following:

$${}_u\omega_{k+1} = {}_u\omega_k + \mu\{F({}_uR_x/L)^{-1}F^{-1}\}\,{}_s\bar{X}_k\,{}_ue_k, \qquad (45)$$

Combining (33) and (45), we finally get a self-orthogonalizing UFBLMS algorithm as

$${}_u\omega_{k+1} = {}_u\omega_k + \eta\,{}_u\Lambda_x^{-1}\,{}_s\bar{X}_k\,{}_ue_k. \qquad (46)$$

As done in [9], the NxN diagonal matrix ${}_u\Lambda_x$ can be computed by first estimating the input autocorrelation values $\{\rho_l\}_{l=0}^{m}$, and then computing either the FFT of the N-point sequence $\{\rho_0, \rho_1, \cdots, \rho_m, 0, \cdots, 0, \rho_m, \cdots, \rho_2, \rho_1\}$ or the eigenvalues represented by (34).

Next we discuss another possible self-orthogonalizing algorithm which is given by

$${}_u\omega_{k+1} = {}_u\omega_k + \gamma\,{}_sR_k^{-1}\,{}_s\bar{X}_k\,{}_ue_k \qquad (47)$$

where ${}_sR_k$ is an NxN diagonal matrix and defined by ${}_sR_k \triangleq E\{{}_s\bar{X}_k\,{}_sX_k\}$ The motivation behind the self-orthogonalizing algorithm in (47) is that the self-orthogonalizing diagonal matrix ${}_sR_k$ can easily be obtained using the transformed input ${}_s\mathcal{X}_k$ which is already available independently of the self-orthogonalization process. To see how the above self-orthogonalizing algorithm works, we derive the mean of the weight-error vector from (17a), (27) and (47) as

$$E[{}_u\mathbf{v}_{k+1}] = (\mathbf{I}_N - \gamma\, {}_s\mathbf{R}_k^{-1}\, {}_u\mathbf{R}_x) E[{}_u\mathbf{v}_k] \tag{48}$$

where ${}_s\mathbf{R}_k \triangleq \mathbf{F}^{-1}\, {}_s\mathcal{R}_k \mathbf{F}$. Since ${}_s\mathcal{X}_k = \mathbf{F}\, {}_s\mathbf{X}_k \mathbf{F}^{-1}$ from (3a) of Part I, we can show from (47) and (48) that

$${}_s\mathbf{R}_k = \mathbf{F}^{-1} E[{}_s\overline{\mathcal{X}}_k\, {}_s\mathcal{X}_k]\mathbf{F} = E[{}_s\mathbf{X}_k^t\, {}_s\mathbf{X}_k]. \tag{49}$$

Comparing (28) and (49), one cannot easily see whether the adjustment algorithm described by (47) and (48) is a self-orthogonalizing algorithm since ${}_s\mathbf{R}_k$ in its present form is not the same as ${}_u\mathbf{R}_x$. However, in the following it will be shown that ${}_s\mathbf{R}_k$ can be approximated and obtained by multiplying ${}_u\mathbf{R}_x$ with a scalar constant.

We can see from (49) that, since ${}_s\mathbf{X}_k$ is circulant, ${}_s\mathbf{R}_k$ is also circulant and symmetric. To compute ${}_s\mathbf{R}_k$ according to (49), we must specify all the elements of ${}_s\mathbf{X}_k$ which is represented by four matrices $\mathbf{X}_a$, $\mathbf{X}_b$, $\mathbf{X}_c$ and $\mathbf{X}_k$. Since $\mathbf{X}_k$ and $\mathbf{X}_c$ are described in (2) and (29) when $N_z = 0$, we specify the elements of the (N-L)xM matrix $\mathbf{X}_a$ and (N-L)x(N-M) matrix $\mathbf{X}_b$ as the following:

$$\mathbf{X}_a = \begin{bmatrix} x_{kL-M-1} & x_{kL+1-1} & \cdots x_{kL-M-L-2} & x_{kL-M-L-1} \\ x_{kL-M-2} & x_{kL-M-1} & \cdots x_{kL-M-L-3} & x_{kL-M-L-2} \\ x_{kL-M-3} & x_{kL-M-2} & \cdots x_{kL-M-L-4} & x_{kL-M-L-3} \\ \vdots & \vdots & \vdots & \vdots \\ x_{kL-2} & x_{kL-3} & \cdots x_{kL-L-1} & x_{kL-L-2} \\ x_{kL-1} & x_{kL-2} & \cdots x_{kL-M-1} & x_{kL-L-1} \end{bmatrix} \tag{50}$$

and

$$\mathbf{X}_b = \begin{bmatrix} x_{kL-M-L} & x_{kL-M-L+1} & \cdots x_{kL-M-3} & x_{kL-M-2} \\ x_{kL-M-L-1} & x_{kL-M-L} & \cdots x_{kL-M-4} & x_{kL-M-3} \\ x_{kL-M-L-2} & x_{kL-M-L-1} & \cdots x_{kL-M-5} & x_{kL-M-4} \\ \vdots & \vdots & \vdots & \vdots \\ x_{kL-L-3} & x_{kL-L-4} & \cdots x_{kL} & x_{kL-1} \\ x_{kL-L-2} & x_{kL-L-3} & \cdots x_{kL-1} & x_{kL} \end{bmatrix} \tag{51}$$

We can now compute the elements of ${}_s\mathbf{R}_k$ from (2),(29),(50) and (51) as

$$({}_s\mathbf{R}_k)_{i,j} = (N-|i-j|)\rho_{|i-j|} + |i-j|\rho_{N-|i-j|}, \quad 1 \leqq i, j \leqq N. \tag{52}$$

Following the same approximation of $|\rho_l|$ used in Section III-B, we can approximate ${}_s\mathbf{R}_k$ as follows. When $m \ll N$, the elements in (52) can first be approximated as

$$({}_s\mathbf{R}_k)_{i,j} = \begin{cases} (N-|i-j|)\rho_{|i-j|}, & 0 \leqq |i-j| \leqq m \\ |i-j|\rho_{N-|i-j|}, & N-m \leqq |i-j| \leqq N-1 \\ 0, & \text{otherwise} \end{cases} \tag{53}$$

Defining a new constant b_l as

$$b_l \triangleq 1 - \frac{l}{N}, \quad 0 \leqq l \leqq m, \tag{54}$$

we can alternatively represent (53) as

$$({}_s\mathbf{R}_k)_{i,j} = \begin{cases} N b_{|i-j|}\rho_{|i-j|}, & 0 \leqq |i-j| \leqq m \\ N b_{N-|i-j|}\rho_{N-|i-j|}, & N-m \leqq |i-j| \leqq N-1 \\ 0, & \text{otherwise.} \end{cases} \tag{55}$$

When $m \ll N$, since $b_l \cong 1$ for $l = 1, 2, \cdots, m$, we can further approximate (55) as

$$({}_s\mathbf{R}_k)_{i,j} = \begin{cases} N\rho_{|i-j|}, & 0 \leqq |i-j| \leqq m \\ N\rho_{N-|i-j|}, & N-m \leqq |i-j| \leqq N-1 \\ 0, & \text{otherwise.} \end{cases} \tag{56}$$

Comparing (32) and (56), we obtain

$${}_s\mathbf{R}_k \cong \frac{N}{L}\, {}_u\mathbf{R}_x. \tag{57}$$

It is noted here that the values of $M(\geqq M_0)$ and m are determined by the signal characteristics. Therefore, once M and m are given, better approximations of both matrices ${}_u\mathbf{R}_x$ and ${}_s\mathbf{R}_k$ are obtained for larger values of L. This is because, as L increases, N increases and thus the validity of the assumption of $m \ll N$ becomes better. Obviously, given M and m, the FLMS case (L=1) results in the worst approximations of ${}_u\mathbf{R}_x$ and ${}_s\mathbf{R}_k$

Substituting (57) into (48), we finally get

$$E[{}_u\mathbf{v}_{k+1}] = (\mathbf{I}_N - \gamma L \frac{1}{N}\, {}_u\mathbf{R}_x^{-1}\, {}_u\mathbf{R}_x)\, E[{}_u\mathbf{v}_k] \tag{58}$$

Based on (44) and (58), we obtain the expressions for the excess MSE's of the two self-orthogonalizing UFBLMS algorithms as

$${}_u\varepsilon_\Delta = \frac{1}{2}\eta\, \mathrm{tr}\,({}_u\mathbf{R}_x^{-1}\, {}_u\mathbf{R}_x)\, {}_u\varepsilon_{min} = \frac{1}{2}\eta N \varepsilon_{min} \tag{59}$$

$${}_u\varepsilon_\Delta = \frac{1}{2}\gamma\, \mathrm{tr}\,(\frac{1}{N}\, {}_u\mathbf{R}_x^{-1}\, {}_u\mathbf{R}_x)\, {}_u\varepsilon_{min} = \frac{1}{2}\gamma \varepsilon_{min} \tag{60}$$

It is noted here that the result on the excess MSE in (60) is independent of the block length L. Comparing (42),(59) and (60), we can have the relation of the convergence constants of the UFBLMS ADF's for the same steady-state MSE as

$$\gamma = \eta N = \mu N \sigma_x^2. \tag{61}$$

In an actual implementation of the self-orthogonalizing UFBLMS algorithm described in (47), ${}_s\boldsymbol{R}_k$ must be estimated in an appropriate way. It has been known that the self-orthogonalizing algorithm using a single-pole LPF for estimation of ${}_s\boldsymbol{R}_k$ significantly improves the convergence speed [1],[5],[9] On the other hand, since the algorithm in (47) is based on the relation between ${}_s\mathbf{R}_k$ and ${}_u\mathbf{R}_x$ in (57), the convergence behavior depends on the accuracy of the approximations of ${}_s\mathbf{R}_k$ and ${}_u\mathbf{R}_x$ As noted earlier in this section, they can be approximated better by processing the signals on the block-by-block basis rather than on the sample-by-sample basis. The improved convergence speed of the self-orghogonalizing FBLMS ADF over the self-orthogonalizing FLMS ADF has been demonstrated in Part I of the paper. It is noted here that in the UFBLMS ADF with M=1 [13]-[18], the two matrices ${}_s\mathbf{R}_k$ and ${}_u\mathbf{R}_x$ are exactly the same. However, as discussed in Section III-D, this structure suffers from the circular convolution effect [20]

B. Self-orthogonalizing Algorithms for Constrained FBLMS ADF

We have shown in Section II-C that the constrained algorithm is derived from the UFBLMS algorithm by placing the constraint on the weight vector. Thus, constrained versions of the two self-orthogonalizing FBLMS ADF's shown in (46) and (47) can be considered as the following:

$${}_s\omega_{k+1} = \boldsymbol{P}_{M,0}\,({}_s\omega_k + \eta\, {}_u\Lambda_x^{-1}\, {}_s\overline{X}_k\, {}_se_k) \tag{62}$$

$${}_s\omega_{k+1} = \boldsymbol{P}_{M,0}\,({}_s\omega_k + \gamma\, {}_s\boldsymbol{R}_k^{-1}\, {}_s\overline{X}_k\, {}_se_k) \tag{63}$$

We first discuss the convergence behavior of the algorithm in (63). The mean of the time-domain weight vector of the algorithm in (63) can be obtained from (19),(20),(26b),(39) and (48) as

$$E[\mathbf{w}_{k+1}] = E[\mathbf{w}_k] + \gamma \mathbf{P}_{M,}\, {}_s\mathbf{R}_k^{-1}\left\{ {}_u\mathbf{R}_x \left[\begin{matrix} {}_B\mathbf{w}_{opt} \\ 0 \end{matrix}\right] - {}_u\mathbf{R}_x \left[\begin{matrix} E[\mathbf{w}_k] \\ 0 \end{matrix}\right] \right\} \tag{64}$$

Thus, we get from (64) the mean of the weight-error vector as

$$E[\mathbf{v}_{k+1}] = E[\mathbf{v}_k] - \gamma \mathbf{P}_{M,}\, {}_s\mathbf{R}_k^{-1}\, {}_u\mathbf{R}_x \left[\begin{matrix} E[\mathbf{v}_k] \\ 0 \end{matrix}\right] \tag{65}$$

Substituting ${}_s\mathbf{R}_k$ of (57) into (65) leads to

$$E[\mathbf{v}_{k+1}] = E[\mathbf{v}_k] - \gamma \mathbf{P}_{M,} \frac{L}{N}\, {}_u\mathbf{R}_x^{-1}\, {}_u\mathbf{R}_x \left[\begin{matrix} E[\mathbf{v}_k] \\ 0 \end{matrix}\right]$$

$$= (\mathbf{I}_M - \gamma L \frac{1}{N} \mathbf{I}_M)\, E[\mathbf{v}_k],$$

Similarly, we can obtain the mean of the weight-error vector of the algorithm in (62) as

$$E[v_{k+1}] = E[v_k] - \eta P_M,\ L_u R_x^{-1}\ _u R_x \begin{bmatrix} E[v_k] \\ 0 \end{bmatrix}$$

$$= (I_M - \eta L I_M) E[v_k], \tag{67}$$

Thus, from (66) and (67) we obtain the excess MSE's of the self-orthogonalizing constrained FBLMS algorithms in (62) and (63) as

$$\varepsilon_\Delta = \frac{1}{2} \eta M \varepsilon_{min} \tag{68}$$

and

$$\varepsilon_\Delta = \frac{1}{2} \gamma \frac{1}{N} M \varepsilon_{min}. \tag{69}$$

Consequently, comparing (9b),(42),(59),(60), (68) and (69), we can see that all the constrained FBLMS algorithms have slightly less steady-state MSE's compared to the corresponding UFBLMS ADF's. The increased excess MSE of the UFBLMS ADF is attributed to the increased effective filter length N in comparison to M of the constrained ADF. Also, we can see the relation in (61) among the convergence constants applies to both cases of the FBLMS ADF's with and without the constraint. The analytical results on the steady-state MSE's of the self-orthogonalizing constrained FBLMS ADF obtained in this section have been demonstrated by computer simulation in Part I of the paper.

V. COMPUTER SIMULATION RESULTS AND DISCUSSION

In the previous sections (and appendix), we have analyzed the convergence behaviors of the unconstrained and self-orthogonalizing FBLMS ADF's. In this section, we present the results of computer simulation to verify the analytical results obtained previously. For our computer simulation, we considered three application examples; adaptive channel equalization, adaptive echo cancellation, and adaptive spectral line enhancement. The adaptive equalizer used here is identical to that in Part I. For the adaptive data echo canceller, the adaptive structure shown in [21, Fig 1] was chosen along with the echo canceller response in [21, Fig. 2] The input of the echo canceller was random binary data and the variance of the noise added at the output was 0.001. On the other hand, the Δ-step adaptive structure in [22, Fig 1] was used for the simulation of the adaptive line enhancer (ALE). In our simulation, the decorrelation delay Δ was set to be unity and the input SNR was -6 dB.

To see the effects of self-orthogonalization and removing the constraint on the convergence behaviors of the FBLMS ADF's when the filter length is sufficiently long, we did simulation of the adaptive equalizer mentioned above. The results are shown in Figs. 2 and 3 for the cases with and without the constraint and the self-orthogonalization operation, respectively. We can see from all those figures that, as analyzed previously, the MSE's of the four unconstrained algorithms increase slightly in comparison to the corresponding constrained algorithms. We can also note that the comparison of the FBLMS ADF's with and without the self-orthogonalization in the frequency domain reveals two distinctive characteristics, one in the transient period and the other in the steady state. We used the same values chosen in Part I for the initial estimate of the self-orthogonalizing matrix for the cases shown in Fig. 3(a) and (b). Unlike the constrained algorithm, the unconstrained algorithm shows an overshoot in the transient period both for the cases of the overlap-save and overlap-add sectioning methods. Therefore, an increased initial estimate must be used in the unconstrained algorithm which is more likely to become unstable because of its increased effective filter length. On the other hand, unlike in the case of the constant convergence factor, the self-orthogonalizing algorithms realized using overlap-add sectioning show increased steady-state MSE's as compared to those realized using overlap-save sectioning

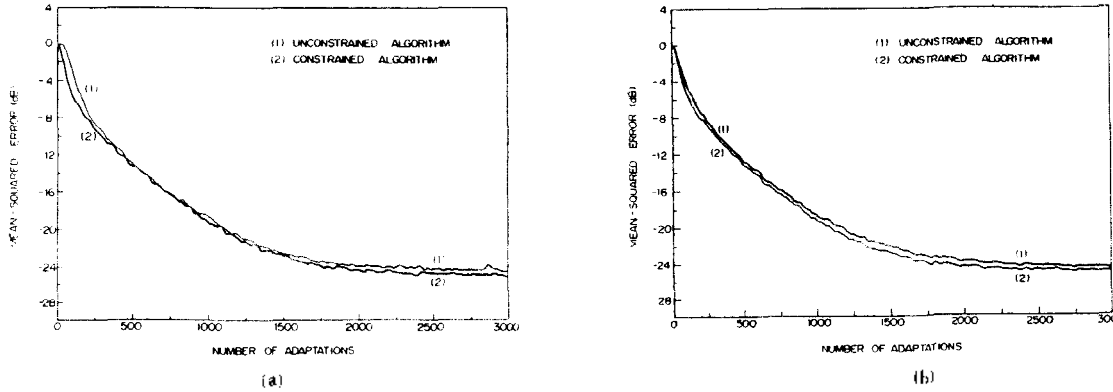

Fig. 2. Comparison of the convergence behaviors of the FBLMS ADF's with the same convergence constant μ for the cases with and without the constraint ($M = 16$, $L = 16$, $N = 32$, $\mu = \alpha / \sigma_x^2$, $\sigma_x^2 = 1.001$ and $\alpha = 0.015$).
(a) Overlap-save sectioning.
(b) Overlap-add sectioning.

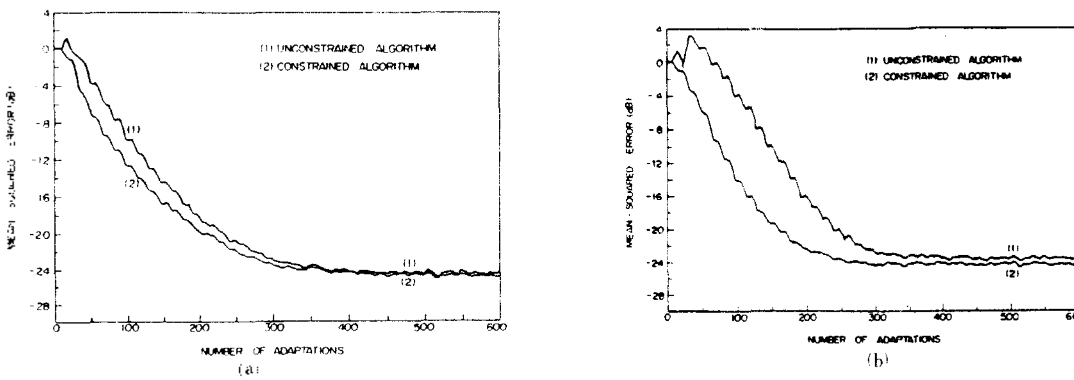

Fig. 3. Comparison of the convergence behaviors of the self-orthogonalizing FBLMS ADF's for the cases with and without the constraint ($M = 16$, $L = 16$, $N = 32$, $\beta = 0.8$, $\gamma = \alpha N$ and $\alpha = 0.015$).
(a) Overlap-save sectioning.
(b) Overlap-add sectioning.

To verify our discussion in Section III on the convergence characteristics of the unconstrained algorithm when the filter length is not sufficiently long, we did computer simulation of an adaptive echo canceller. In Fig. 4 we first show what values the weights of the FBLMS ADF's with and without the constraint have eventually in the steady state. We can see from Fig. 4(a) and (b) that, unlike the constrained algorithm, some of the last (N-M) weights of the unconstrained algorithm are not zero in the steady state, although the first M weights of the two filters are about the same. Comparing Fig. 4(b) with the original echo channel response, it turns out that they are very close to each other [21]. In Fig 5 we show the MSE behaviors of the same ADF's. We can see from this figure that, as discussed in Section III, the unconstrained algorithm reveals degradation in MSE in the beginning of the block due to the circular convolution effect. However, in the rest of the block, the MSE performance is significantly

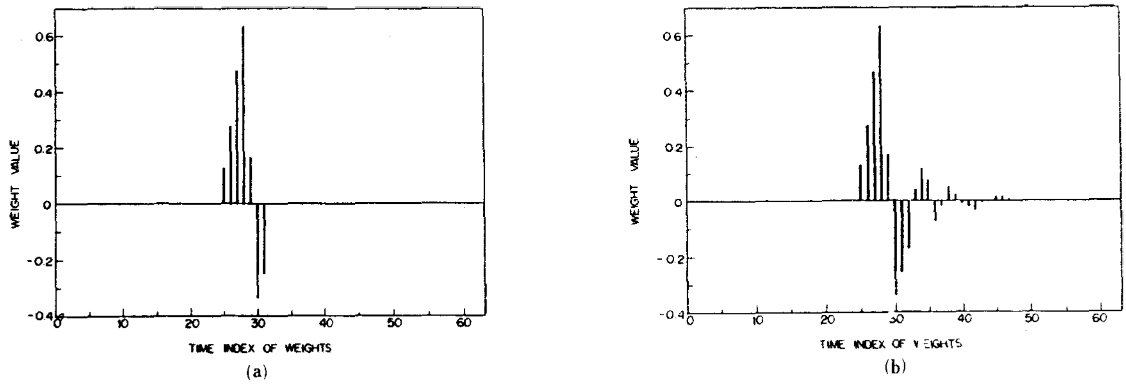

Fig. 4. Comparison of the steady-state weight values of the FBLMS ADF's with and without the constraint when the filter length is not sufficient (M=32, L=32, N=64, and μ=0.01)
(a) Constrained algorithm.
(b) Unconstrained algorithm.

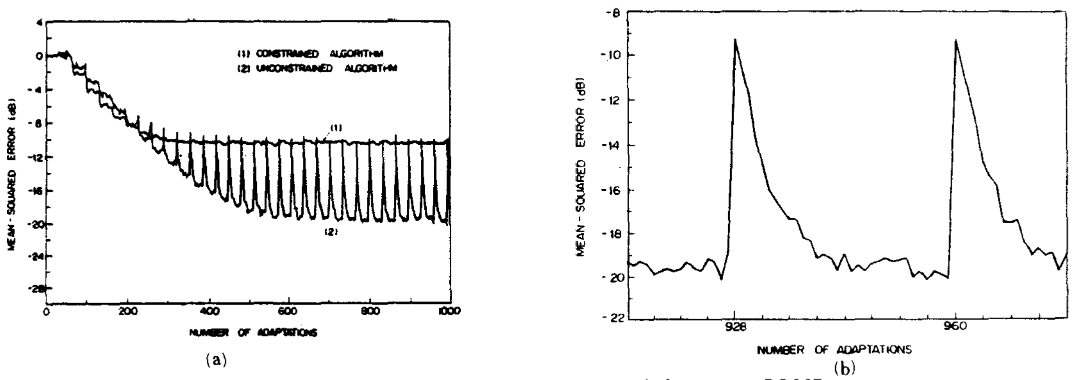

Fig. 5. Comparison of the MSE's of the same FBLMS ADF's used in Fig. 4.
(a) Overall convergence behaviors.
(b) Convergence behavior of the UFBLMS ADF in the 30th block.

improved by having nonzero values after the M_{th} weight. Consequently, in that way the unconstrained algorithm minimizes the overall block MSE which can be much less than that of the constrained algorithm.

Finally, we discuss the results of computer simulation of the ALE with $\Delta=1$. In Fig. 6(a) and (b), we show the time-domain weight values of the two FBLMS ALE's in the steady state. We see from this figure that the UFBLMS ALE has a very large peak in its time-domain response. The reason is as follows. Based on the representations of the output and data matrices shown in (43),(2) and (29), respectively, the desired response vector of the UFBLMS ALE with $\Delta=1$ is given as $d_k=[x_{kL+1}\ x_{kL+2}\cdots x_{kL+L-1}\ x_{kL+L}]^t$. Thus, we can see from (29) that the last column of X_c is almost the same as d_k. Consequently, we can see from (43) that, to minimize the MSE between y_k and d_k, the last element of the weight vector $_u w_k$ must be very large. However, it is interesting to see from Fig. 6(a) and (b) that the first M weights of the two ALE's appear to have similar information. Those weights are different only by a scale factor. This aspect can be seen more clearly in the frequency responses of Fig. 6(c). As an extreme case of the UFBLMS ALE, we can consider the

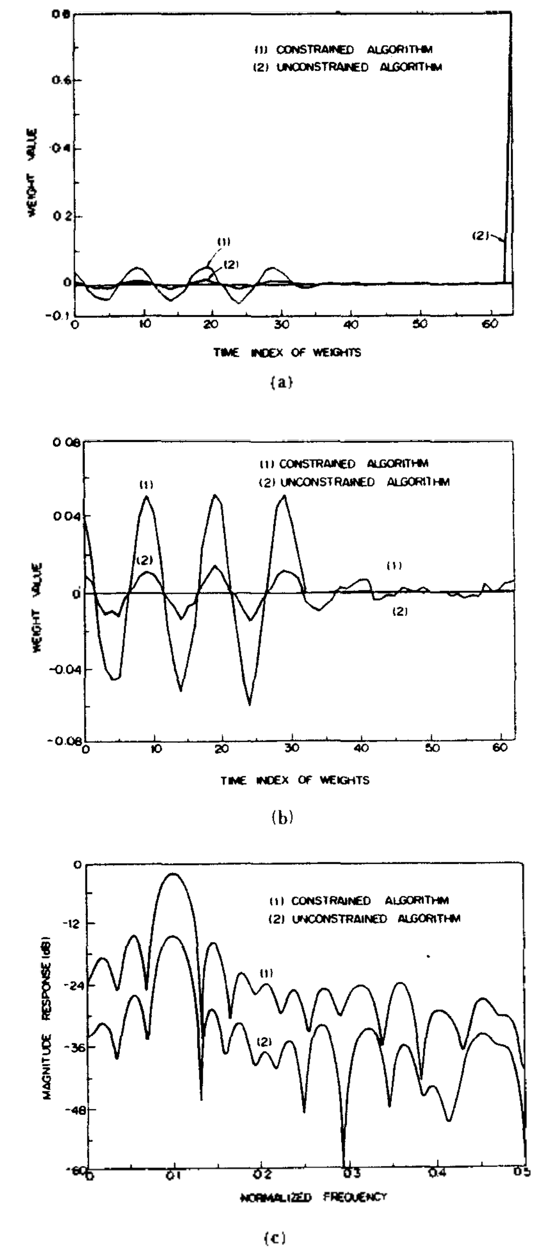

Fig. 6. Comparison of the steady-state performances of the FBLMS ALE's with and without the constraint (M=32, L=32, N=64, μ =0.0001 and the normalized frequency of the sinusoid, $\bar{f}_o$ =0.1).

(a) Overall N time-domain weight values $\{w_i\}_{i=0}^{N-1}$.

(b) First (N-1) time-domain weight values $\{w_i\}_{i=0}^{N-2}$.

(c) Magnitude frequency responses of the weights in (b).

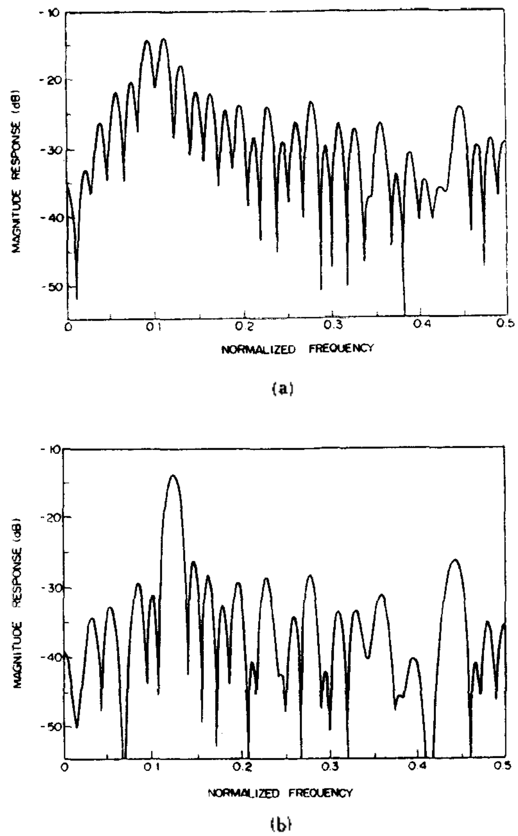

Fig. 7. Frequency responses of the UFBLMS ALE with M=1 for different frequencies of the input sinusoid (M=1, L=64, N=64 and μ = 0.0001).

(a) $\bar{f}_o = 0.1$ (b) $\bar{f}_o = 0.125$

case when M=1 and thus N=L, which is the same structure as that studied in [13]-[18]. The frequency response of the first (N-1) time-domain weights is shown in Fig. 7(a). As noted in Section III, the performance, however, appears to be unsatisfactory. As can be seen in Fig. 7(b), the frequency response may be improved for a different input frequency because of the periodic nature of the sinusoid when the input SNR is high. It is noted that all those frequency responses of the UFBLMS ALE discussed so far have been obtained by removing the peak in the time-domain response. This means that in the ALE's we cannot expect the same computational saving that has been gained in other applications by removing the constraint on the weights.

VI. CONCLUSIONS

In Part I of the paper, both for the cases of the overlap-save and overlap-add sectioning we derived the unconstrained algorithms from the alternative structures which cannot be obtained directly from the original BLMS ADF. The reason for doing so was as follows. According to our simulation result, unlike the conventional FBLMS ADF derived from the BLMS ADF, both the alternative and unconstrained FBLMS ADF's always converge to the optimum Wiener solution for any initial values of the frequency-domain weight vector. In Part II we have shown that the UFBLMS ADF is basically a frequency-domain problem for which case the optimum solution must be formulated directly in the frequency domain. Also, it has been shown that the autocorrelation matrix governing the convergence behavior of the UFBLMS ADF's is approximately a diagonal matrix in the frequency domain (or a circulant matrix in the time domain) both for the cases of the overlap-save and over-lap-add sectioning. Furthermore, we have shown that the convergence behavior of the self-orthogonalizing FBLMS ADF with the constraint is governed by the same autocorrelation matrix as that of the FBLMS ADF without the constraint. Therefore, we believe that the UFBLMS ADF must be conceived as an independent problem and thereafter a constrained version of the UFBLMS ADF could be considered as a special case with the constraint on the weights if it is necessary such as in the Δ-step linear prediction.

In this paper, we have analyzed extensively the convergence behaviors of the UFBLMS and self-orthogonalizing FBLMS ADF's realized based on overlap-save sectioning. According to the results of our analysis, the optimum solutions of the two FBLMS ADF's with and without the constraint are the same when $M \geq M_o$. The mean of the weight vector of the UFBLMS ADF has also been shown to converge to the optimum solution regardless of the initial values of the frequency-domain weight vector. It has been shown by analysis that the steady-state MSE of the UFBLMS ADF, however, increases slightly in comparison to the constrained algorithm when the same convergence constant is used in both cases. On the other hand, when $M < M_o$, the original and unconstrained FBLMS ADF's have been shown to reveal quite different convergence behaviors in the steady state. It has been found that, when $M < M_o$, the UFBLMS ADF suffers from the circular convolution effect in the first $M - M_o$ output samples in each block. However, in the rest output samples in the block, while the constrained algorithm yields poor performance due to the insufficient filter length, the performance of the UFBLMS ADF is improved significantly by utilizing its extended filter-length capability. As another new result, we have shown by computer simulation that the UFBLMS ADF used even in the adaptive line enhancer application has the same information about the signals as the constrained algorithm does. Consequently, in most applications the use of the UFBLMS algorithms yields no significant degradation in performance.

As for the self-orthogonalizing FBLMS ADF, we have studied in detail the properties of the autocorrelation matrix and the self-orthogonalizing matrix. As a result, we have shown that the two matrices can be approximated such that they differ only by a constant scale factor. It has also been shown that the accuracy of the approximations of these matrices can be improved when the block length is sufficiently long. This result verifies why the self-orthogonalizing FBLMS ADF can have superior convergence speed over the self-orthogonalizing FLMS ADF which operates on a sample-by-sample basis. In addition, we have obtained the analytical results on the steady-state MSE's of the self-orthogonalizing FBLMS ADF's with and without the constraint and verified the relations among the convergence factors that were suggested in Part I. Finally, in Appendix we have analyzed the convergence behavior of the overlap-add implementation. According to the result obtained, it has been found that the excess MSE of the self-orthogonalizing FBLMS ADF using overlap-add sectioning is larger than that of the overlap-save implementation for the same convergence constant.

APPENDIX

Convergence Analysis of FBLMS ADF's Realized Using Overlap-add Sectioning

In this appendix, we analyze the convergence behavior of the overlap-add I implementation developed in Part I of the paper. This appendix together with Sections III and IV which dealt with the convergence behavior of the overlap-save implementation will provide a unified theory on the convergence behaviors of the FBLMS ADF's realized based on the fast convolution.

A. Unconstrained Algorithm

The frequency-domain error vector of the overlap-add implementation is defined from (37) of Part I as

$$ {}_u e_k \triangleq {}_a d_k - (P_{L,0}\,{}_a X_k + Q_{L,0}\,{}_a \overline{X}_{k-1})\,{}_u \omega_k \,. \qquad (A.1) $$

The pair of the FBLMS ADF's based on overlap-add I sectioning is given as

$$ {}_u \omega_{k+1} = {}_u \omega_k + \mu\,({}_a \overline{X}_k\,{}_u e_k + {}_a \overline{X}_{k-1}\,{}_u e_k) \qquad (A.2) $$

and

$$ {}_a \omega_{k+1} = P_{M,0}[\,{}_a \omega_k + \mu\,({}_a \overline{X}_k\,{}_a e_k + {}_a \overline{X}_{k-1}\,{}_a \acute{e}_k)] \qquad (A.3) $$

where ${}_u \acute{e}_k = Q^*_{L,0}\,{}_u e_k$. The optimum weight vector ${}_u \omega_{opt}$ of the UFLMS ADF in (A.2) must satisfy

$$ E[\,{}_a \overline{X}_k\,{}_u e_k + {}_a \overline{X}_{k-1}\,{}_u \acute{e}_k] = 0 \qquad (A.4) $$

Substituting (A.1) into (A.4) yields

$$ E[({}_a \overline{X}_k P_{L,0} + {}_a \overline{X}_{k-1} Q^*_{L,0})\,{}_a d_k] \qquad (A.5) $$
$$ = E[({}_a \overline{X}_k P_{L,0} + {}_a \overline{X}_{k-1} Q^*_{L,0})(P_{L,0}\,{}_a X_k + Q_{L,0}\,{}_a X_{k-1})] $$
$$ {}_u \omega_{opt} $$

Converting all the variables from the frequency domain into the time domain, we get

$$ E[({}_a \mathbf{X}_k^t \mathbf{P}_{L,0} + {}_a \mathbf{X}_{k-1}^t \mathbf{S}_{M-1,0})\,{}_a \mathbf{d}_k] \qquad (A.6) $$
$$ = E[({}_a \mathbf{X}_k^t \mathbf{P}_{L,0} + {}_a \mathbf{X}_{k-1}^t \mathbf{S}_{M-1,0})(\mathbf{P}_{L,0}\,{}_a \mathbf{X}_k + \mathbf{Q}_{L,0}\,{}_a \mathbf{X}_{k-1})] $$
$$ {}_u \mathbf{w}_{opt} \,. $$

Using the definitions of ${}_a \mathbf{X}_k$, $\mathbf{P}_{L,0}$ and $\mathbf{Q}_{L,0}$, we can show that

$$ \mathbf{P}_{L,0}\,{}_a \mathbf{X}_k + \mathbf{Q}_{L,0}\,{}_a \mathbf{X}_{k-1} = \begin{bmatrix} {}_s \mathbf{X}_u \\ \mathbf{0} \end{bmatrix} \begin{matrix} L \\ N-L \end{matrix} \,. \qquad (A.7) $$

Thus, we get from (A.6) and (A.7)

$$ E[\,{}_s \mathbf{X}_u^t\,\mathbf{d}_k] = E[\,{}_s \mathbf{X}_u^t\,{}_s \mathbf{X}_u]\,{}_u \mathbf{w}_{opt} \,. \qquad (A.8) $$

Comparing (A.8) and (26b), we can see that the optimum weight vectors of the two UFBLMS ADF's are the same both for the overlap-save and overlap-add I implementations. In other words, the overlap-add I implementation in (A.2) is another exact implementation of the system described by (22a) and (22b). Consequently, the same results on the convergence behavior obtained in Section III apply to the overlap-add implementation with a constant convergence factor as well. However, it will be seen in the following that this is not the case when the weight-adjustment algorithm is modified using the frequency-domain self-orthogonalizing matrix.

B. Self-orthogonalizing Algorithm

We discuss the following self-orthogonalizing algorithms in order:

$$ {}_u \omega_{k+1} = {}_u \omega_k + \mu\,({}_a R_k^{-1}\,{}_a \overline{X}_k\,{}_u e_k + {}_a R_k^{-1}\,{}_a \overline{X}_{k-1}\,{}_u \acute{e}_k) \qquad (A.9) $$

and

$$ {}_a \omega_{k+1} = P_{M,0}[\,{}_a \omega_k + \mu\,({}_a R_k^{-1}\,{}_a \overline{X}_k\,{}_a e_k + {}_a R_k^{-1}\,{}_a \overline{X}_{k-1}\,{}_a \acute{e}_k)] \,. \qquad (A.10) $$

where the NxN diagonal matrix $_a\mathcal{R}_k$ is defined as $_a\mathcal{R}_k \triangleq E[_a\bar{\mathcal{X}}_k\,{}_a\mathcal{X}_k]$. Following the same approach as used in the previous subsection, we can get the following for (A.9) as

$$E[_u w_{k+1}] = E[_u w_k] + \gamma E[(_a R_k^{-1}\,{}_a X_k^t P_{L,o} + {}_a R_{k-1}^{-1}\,{}_a X_{k-1}^t\ S_{M-1,o}) \{_a d_k - (P_{L,o}\,{}_a X_k + Q_{L,o}\,{}_a X_{k-1})\,{}_u w_k\}] \qquad (A.11)$$

where

$$_a R_k \triangleq F^{-1}\,{}_a\mathcal{R}_k\,F.$$

when $d_k = X_k w_d + \xi_k$, we can show that

$$d_k = {}_s X_u \begin{bmatrix} w_d \\ O \end{bmatrix} + \xi_k = {}_s X_u\,{}_u w_{opt} + \xi_k. \qquad (A.12)$$

Combining (A.7), (A.8), (A.11) and (A.12), we obtain

$$E[_u v_{k+1}] = (I_N - \gamma R_v) E[_u v_k] \qquad (A.1\ )$$

where

$$R_v \triangleq E[(_a R_k^{-1}\,{}_a X_k^t P_{L,o} + {}_a R_{k-1}^{-1}\,{}_a X_{k-1}^t\ S_{M-1,o}) (P_{L,o}\,{}_a X_k + Q_{L,o}\,{}_a X_{k-1})].$$

Expanding R_v into two terms leads to

$$R_v = {}_a R_k^{-1}\ E[_a X_k^t\ P_{L,o}(P_{L,o}\,{}_a X_k + Q_{L,o}\,{}_a X_{k-1})] + {}_a R_{k-1}^{-1}\ E[_a X_{k-1}^t\ S_{M-1,o}(P_{L,o}\,{}_a X_k + Q_{L,o}\,{}_a X_{k-1})]. \qquad (A.14)$$

Noting that the correlation values between input samples of the different blocks are very small when $L \gg m$, we can approximate R_v in (A.14) as

$$R_v = {}_a R_k^{-1} E[(P_{L,o}\,{}_a X_k)^t (P_{L,o}\,{}_a X_k)] + {}_a R_{k-1}^{-1} E[(Q_{L,o}\,{}_a X_{k-1})^t (Q_{L,o}\,{}_a X_{k-1})]. \qquad (A.15)$$

In the steady state, R_v becomes

$$R_v = {}_a R_k^{-1}\ E[(P_{L,o}\,{}_a X_k)^t (P_{L,o}\,{}_a X_k) + (Q_{L,o}\,{}_a X_{k-1})^t (Q_{L,o}\,{}_a X_{k-1})] \qquad (A.16)$$

$$= {}_a R_k^{-1}\ E[(P_{L,o}\,{}_a X_k)^t (P_{L,o}\,{}_a X_k) + (Q_{L,o}\,{}_a X_{k-1})^t (Q_{L,o}\,{}_a X_{k-1})].$$

Denoting ${}_a X_k \triangleq \begin{bmatrix} A \\ B \end{bmatrix}\begin{matrix} L \\ N-L \end{matrix}$, we can modify (A.16) as

$$R_v = {}_a R_k^{-1}\ E[A^t A + B^t B]$$

$$= {}_a R_k^{-1}\ E[\begin{bmatrix} A \\ B \end{bmatrix}^t \begin{bmatrix} A \\ B \end{bmatrix}] = {}_a R_k^{-1}\ E[_a X_k^t\,{}_a X_k]. \qquad (A.17)$$

We finally get from (A.13) and (A.17)

$$E[_u v_{k+1}] = (I_N - \gamma\,{}_a R_k^{-1}\,{}_a R_k) E[_u v_k]. \qquad (A.18)$$

Consequently, the excess MSE of the self-orthogonalizing algorithm in (A.9) is given as

$$_u\varepsilon_\Delta = \frac{1}{2}\gamma\frac{N}{L}\varepsilon_{min}. \qquad (A.19)$$

As for the constrained self-orthogonalizing FBLMS ADF of (A.10), we can get

$$E[v_{k+1}] = E[v_k] - \gamma P_{M,}\,{}_a R_k^{-1}\,{}_a R_k \begin{bmatrix} E[v_k] \\ O \end{bmatrix}\begin{matrix} M \\ N-N \end{matrix}$$

$$= (I_M - \gamma I_M) E[v_k] \qquad (A.20)$$

Thus, the excess MSE of (A.10) becomes from (A.20)

$$\varepsilon_\Delta = \frac{1}{2}\gamma\frac{M}{L}\varepsilon_{min}. \qquad (A.21)$$

Comparing (A.19) and (A.21) with (60) and (69), respectively, we can see that the excess MSE's of the self-orthogonlizing FBLMS ADF's realized using overlap-add sectioning are larger than those of the overlap-save implementation when the same convergence constants are used in both cases.

REFERENCES

1. J.C. Lee and C.K. Un, "Time- and frequency-domain block LMS adaptive digital filters: Part I – Realization structures," Journal of Acoust. Society of Korea, this issue.
2. G.A. Clark, "Block adaptive filtering and its application to seismic event detection," Ph.D. dissertation, Univ. California, Santa Barbara, CA, Apr. 1981.
3. G.A. Clark, S.K. Mitra, and S.R. Parker, "Block implementation of adaptive digital filters," IEEE Trans. Acoust., Speech, Signal Processing, vol. ASSP-29, pp.744-752, June 1981.
4. B. Widrow and S.D. Stearns, *Adaptive Signal Processing.* Englewood Cliffs, NJ: Prentice-Hall, 1985.
5. D. Mansour and A.H. Gray, Jr., "Unconstrained frequency-domain adaptive filter," IEEE Trans. Acoust., Speech, Signal Processing, vol. ASSP-30, pp.726-734, Oct. 1982.
6. D. Mansour and A.H. Gray, Jr., "Performance characteristics of the unconstrained frequency-domain adaptive filter," in Proc. 1982 IEEE Int. Symp. Circuits Syst., May 1982, pp.695-698.
7. G. Picchi and G. Prati, "Self-orthogonalizing adaptive equalization in the discrete frequency domain," IEEE Trans. Commun., vol. COM-32, pp.371-379, Apr. 1984.
8. J.B. Rosen, "The gradient projection method for non-linear programming," SIAM J. Appl. Math., pp.181-218, March 1960.
9. J.C. Lee and C.K. Un, "Performance of transform-domain LMS adaptive digital filters," IEEE Trans. Acoust., Speech, Signal Processing, vol. ASSP-34, pp.499-510, June 1986.
10. H.C. Andrews and B.R. Hunt, *Digital Image Restoration.* Englewood Cliffs, NJ: Prentice-Hall, 1977.
11. J.C. Lee, "A class of adaptive digital filters and their applications," Ph.D. dissertation, Dept. Elec. Eng., Korea Advanced Inst. Sci. Technol., Seoul, Korea, June 1983.
12. G.A. Clark, S.R. Parker, and S.K. Mitra, "A unified approach to time- and frequency-domain realization of FIR adaptive digital filters," IEEE Trans. Acoust., Speech, Signal Processing, vol. ASSP-31, pp.1073-1083, Oct. 1983.
13. M.J. Dentino, J. McCool, and B. Widrow, "Adaptive filtering in the frequency domain," Proc. IEEE, vol. 66, pp.1658-1659, Dec. 1978.
14. N.J. Bershad and P.L. Feintuch, "Analysis of the frequency domain adaptive filter," Proc. IEEE, vol. 67, pp.1658-1659, Dec. 1979.
15. F.A. Reed and P.L. Feintuch, "A comparison of LMS adaptive cancellers implemented in the frequency domain and the time domain," IEEE Trans. Acoust., Speech, Signal Processing, vol. ASSP-29, pp.770-775, June 1981.
16. J.C. Ogue, T. Saito, and Y. Hoshiko, "A fast convergence frequency domain adaptive filter," IEEE Trans. Acoust., Speech, Signal Processing, vol. ASSP-31, pp.1312-1314, Oct. 1983.
17. A. Morgul, P.M. Grant, and C.F.N. Cowan, "Wide-band hybrid analog/digital frequency domain adaptive filter," IEEE Trans. Acoust., Speech. Signal Processing, vol. ASSP-32, pp.762-769, Aug. 1984.
18. F.A. Reed, P.L. Feintuch, and N.J. Bershad, "The application of the frequency domain LMS adaptive filter to split array bearing estimation with a sinusoidal signal," IEEE Trans. Acoust., Speech, Signal Processing, vol. ASSP-23, pp.61-69, Feb. 1985.
19. R.D. Gitlin and F.R. Magee, Jr., "Self-orthogonalizing adaptive equalization algorithms," IEEE Trans. Commun., vol. COM-25, pp.666-672, July 1977.
20. E.R. Ferrara, Jr., "Frequency-domain adaptive filtering," in *Adaptive Filters,* C.F.N. Cowan and P.M. Grant, Eds. Englewood Cliffs, NJ: Prentice-Hall, 1985.
21. D.L. Duttweilter, "Subsampling to estimate delay with application to echo cancelling," IEEE Trans. Acoust., Speech, Signal Processing, vol. ASSP-31, pp.1090-1099, Oct. 1983.
22. J.R. Treichler, "Transient and convergent behavior of the adaptive line enhancer," IEEE Trans. Acoust., Speech, Signal Processing, vol. ASSP-27, pp.53-62, Feb. 1979.

▲ **Jae Chon Lee** was born in Seoul, Korea, in 1954. He received the B.S. degree with honors in electronics engineering from Seoul National University (SNU), Seoul, in 1977, and the M.S. and Ph.D. degrees in electrical engineering from the Korea Advanced Institute of Science and Technology (KAIST), Seoul, in 1979 and 1983, respectively.

Since August 1983, he has been with KAIST as a senior research scientist. During the academic years 1984-1985 and 1985-1986, he was on leave at the Massachusetts Institute of Technology (MIT) and the University of California at Santa Barbara (UCSB), working with Prof. Jae Lim and Prof. Sanjit Mitra, respectively. His research interest is in the area of digital signal processing and digital communication systems including adaptive filtering and neural computing.

▲ **Dr. Chong Kwan Un** received the B.S., M.S., and Ph.D. degrees in electrical engineering from the University of Delaware, Newark, Delaware, in 1964, and 1969, respectively. From 1969 to 1973 he was Assistant Professor of Electrical Engineering at the University of Maine, Portland, where he taught communications and did research on synchronization problems. In May 1973, he joined the Staff o the Telecommunication Sciences Center, SRI International, Menlo Park, CA, where he did research on voice digitization and bandwidth compression systems. Since June 1977 he has been with KAIST, where he is Professor of Electrical Engineering and Head of the Communications Research Laboratory, teaching and doing research in the areas of digital communications and digital signal processing. He has authored or coauthored over 140 papers and 50 reports in speech coding and processing, packet voice/data transmission, synchronization, and digital filtering. Also, he holds 6 patents granted or pending. From February 1982 to June 1983 he served as Dean of Engineering at KAIST.

Dr. Un has received a number of awards including the 1976 Best Paper Award from the IEEE Communications Society, the National Order of Merits (Dong Baik Jang) from the Government of Korea, and Achievement Awards from KITE, KICS and ASK. He is a Fellow of IEEE and a member of Tau Beta Pi and Eta Kappa Nu Honor Societies.